Pergamon

Bioorganic & Medicinal Chemistry, Vol. 4, No. 9, pp 1565–1572, 1996

PII: S0968-0896(96)00149-6
0968-0896/96 $15.00+0.00

Solution Conformations of KNI-272, a Tripeptide HIV Protease Inhibitor Designed on the Basis of Substrate Transition State: Determined by NMR Spectroscopy and Simulated Annealing Calculations

Yasushi Ohno,[a] Yoshiaki Kiso[b] and Yuji Kobayashi[a,*]

[a]*Institute for Protein Research and Faculty of Pharmaceutical Research, Osaka University, Suita, Osaka 565, Japan*
[b]*Department of Medicinal Chemistry, Kyoto Pharmaceutical University, Yamashina-ku, Kyoto 607, Japan*

Abstract—KNI-272, a highly selective and potent HIV protease inhibitor containing allophenylnorstatine [(2*S*,3*S*)-3-amino-2-hydroxy-4-phenylbutyric acid], named Apns, has been studied in dimethylsulfoxide-d_6 by NMR spectroscopy and simulated annealing calculations. ^{1}H and ^{13}C spectra showed the presence of two conformers characterized by the configuration of the imide bond between the Apns and Thz residues, i.e., *trans* and *cis* forms, respectively. Rotating frame Overhauser effect spectra revealed that the *trans* conformer is dominant. The solution structure calculated from the distance information resulting from nuclear Overhauser effects experiments is similar overall to those observed in the solid states, either as a single crystal or as complex with the protease. The results from both molecular dynamics simulations and experimental ^{13}C longitudinal relaxation times indicate that the backbone of KNI-272 has a fairly rigid conformation. Copyright © 1996 Elsevier Science Ltd

Introduction

One of the most active areas of drug discovery in the world today concerns therapies for AIDS. The human immunodeficiency virus (HIV-1), which is the causative agent of this disease, codes for an aspartic protease known to be essential for retroviral maturation and replication. The HIV-1 protease recognizes Phe–Pro and Tyr–Pro sequences (Fig. 1) as the virus-specific cleavage site, but mammalian aspartic proteases do not have this specificity. These features provided a basis for the rational design of selective HIV protease-targeted drugs or inhibitors for the treatment of AIDS and its related complex.

The transition state of amide hydrolysis by an aspartic protease is proposed, as illustrated in Figure 1. The hydrogen bond between the carboxylic acid of protease and the hydroxyl group of the substrate transition state is very important in the design of tight-binding inhibitors. Based on the substrate transition-state mimetic concept, we designed and synthesized a novel class of HIV protease inhibitors containing an unnatural amino acid, (2*S*,3*S*-)-3-amino-2-hydroxy-4-phenylbutyric acid, named allophenylnorstatine (Apns),[1,2] with a hydroxymethylcarbonyl isostere.[3] After identifying the tripetide derivative KNI-102 (Z-Asn-Apns-Pro-NHBu^t, Z = benzyloxycarbonyl)[2] as a lead compound, we undertook to further optimize this lead and found a highly selective and potent HIV protease inhibitor, KNI-272 (iQoa-Mta-Apns-Thz-NHBu^t, iQoa = isoquinolinyloxyacetyl, Mta = methylthioalanine, Thz = thiazolidine-4-carboxylic acid, thioproline, Fig. 1).[1] Both the hydroxyl group and the carbonyl group of Apns as a transition state mimic interact with the aspartic acid carboxyl groups of the HIV protease active site, and the stereochemistry of this hydroxyl group is necessary for the inhibitory activity.[1,2,4–6]

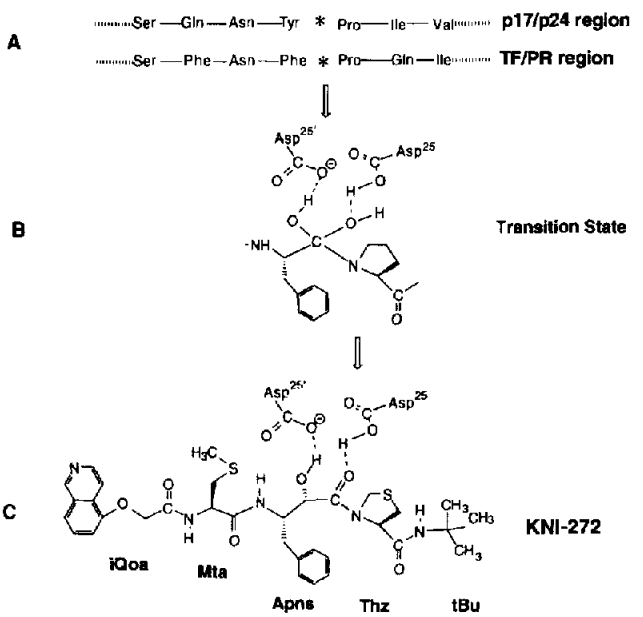

Figure 1. Design of KNI-272 based on substrate transition state. (A) Substrate for HIV-1 protease. (B) Substrate transition state in the active site of HIV protease. (C) KNI-272 in the active site of HIV protease. Abbreviations are as follows: p17/p24, 17K protein/24K protein; TF/PR, transframe protein/protease; iQoa, 5-isoquinolylacetic acid; Mta, methylthioalanine; Apns, allophenylnorstatine; Thz, thioproline; Bu^t, *tert*-butylamine.

KNI-272 has been shown to be a selective and potent inhibitor of HIV protease, with an inhibitory constant (K_i) of 5.5 pM, that posses potent anti-HIV activity with low cytotoxity.[4] An oral formulation of KNI-272 has recently entered clinical trials for the treatment AIDS.

Doi et al.[5] studied the crystal structure of KNI-272 and compared it with its bound conformation in the protease complex as reported by Baldwin et al.[6] They reported that all the single crystal structures obtained from various solvents were similar to the bound structure. They also put forth the hypothesis that KNI-272 may be constrained and 'preorganized' in its bioactive conformation. This fact led us to examine the conformation of KNI-272 in solution.

Flexible ligands generally change their conformations upon binding to an enzyme. This is especially true for molecules with five or six rotatable bonds. Usually neither the NMR nor the crystal structure represents the binding conformation and shape well.[7] If the solution structure of KNI-272 is similar to the crystal structure, then the 'preorganized' hypothesis would be supported and validated. In this paper, we will report the conformation of KNI-272 in solution, and compare this conformation with those observed previously in the solid states, both as a crystal[5] and as a complex with the protease.[6]

Results

Assignment of NMR signals

The assignment of all protons was done using the DQFCOSY and NOESY spectra (Table 1). Those of carbon nuclei directly bound to protons were assigned either from a ^1H ^{13}C HMQC spectrum for carbons or from a ^1H ^{13}C HMBC spectrum for all the remaining (Table 2).

^1H and ^{13}C NMR spectra showed that KNI-272 takes two distinct isomeric forms in DMSO-d_6. At the imide bond, between the Apns and the Thz residue, a slow *cis–trans* interconversion would be expected to cause such isomerism. Generally, the configuration for Xxx-Pro imide bonds is distinguished by the fact that the *cis* form allows much close contact between the $C_\alpha H$ proton of Xxx and the $C_\alpha H$ proton of the following Pro. On the other hand, the *trans* form favors a short distance between the $C_\alpha H$ proton of Xxx and the $^\delta CH$ proton of the following Pro.[8] The ROESY measurement, which differentiates NOE and chemical exchange, makes it possible to assign the signals corresponding to the *trans* and *cis* forms. Figure 2 displays the mid-field region of the ROESY spectra. For the *trans* isomer, strong ROE cross peaks between the Apns $H_{\beta 2}$ and the Thz H_δ protons were observed around the Apns—Thz imide bond. For the *cis* isomer strong peaks were observed between the Apns H_{b2} and Thzα protons.

Although a low population of *cis* isomer and overlapping signal prevented a detailed analysis of its NMR parameters, the ROESY spectra clearly showed that the isomerism is attributed to slowly interconverting rotormers about the imide bond and the major isomer is in the energetically favorable *trans* form (ca. 85:15). This is consistent with the fact that the *trans* isomers is the more prevalent conformation in both the pure crystal and the bound or complexed state.

Chemical shift dependence on temperature and concentration

The temperature coefficients of the Mta, Apns, and Bu^t amide protons were −5.3, −8.0, and −7.0 ppb/K, respectively, indicating the absence of hydrogen bonding involving these amide groups. Furthermore, the linear temperature dependencies of the chemical shifts for these protons suggests that no major conformational rearrangements occur on the NMR time scale over the temperature range studied.

The possibility of molecular aggregation was examined by comparing ^1H 1-D spectra recorded at various concentrations (1–100 mM). No significant changes in chemical shifts or line width were observed over this range of concentration.

Coupling constants and stereospecific assignments

The vicinal NH—CH_x coupling constants were measured directly from 1-D ^1H spectra (Table 3). These values indicate that the ϕ angle in both Mta and Apns is restricted to the range from −160 to −80°. The CH_α—CH_β coupling constants were measured from the corresponding cross peaks in the ECOSY spectra (Table 3). Generally the χ_1 angle can be estimated to be −60° when both $^3J_{\alpha\beta}$ and $^3J_{\alpha\beta}$ are small (both should be around 3 Hz). If one of $^3J_{\alpha\beta}$ is large (>11 Hz) and the other is small, χ_1 can take either of 60 or 180°. Actually $^3J_{\alpha\beta}$ for Mta shows an intermediate value, indicating motional averaging of the thio methyl group. $^3J_{\alpha\beta}$ for Apns reveals no motional averaging, but

Table 1. ^1H chemical shifts for KNI-272 in DMSO-d_2 solution at 293 K

	Residue	NH	H_α	α_b	Others
1	iQoa		4.65		1H, 9.28, 3H 8.52, 4H 8.05, 6H 7.16, 7H 7.56, 8H 7.69
2	Mta	8.20	4.56	2.73, 2.82	$C_\gamma H_3$ 2.02
3	Apns	8.31	4.15	2.69, 2.75	2,6H 7.32, 3,5H 7.16, 4H 7.08, $C_{\beta 2}H$ 4.46, OH 5.24
4	Thz		4.75	2.97, 3.31	$C_\delta H_2$ 4.64, 4.95
5	*t*Bu	7.70			$C_\beta H_3$ 1.24

the signal overlap of two β protons made it impossible to evaluate any NOEs between NH and the two $C_\beta H$. Therefore, a stereo-specific assignment could not be done for either Mta or the Apns residues.

^{13}C Longitudinal relaxation times (T_1)

Information about the structural flexibility of KNI-272 can be obtained from ^{13}C longitudinal relaxation times (T_1). The NT_1 values (N = number of attached protons) correlate directly with the molecular mobility. This is due to the fact that the ^{13}C relaxation of these carbons is predominantly from a single relaxation mechanism, that is, primarily form $^{13}C—^1H$ dipolar interaction of directly bonded hydrogen atoms.[9] The T_1s determined by inversion-recovery experiments for each of the ^{13}C signals are given in Table 2. The relaxation time (T_1) at the carbonyl carbon of Mta and the NT_1 at the C_α carbon of Apns residue are smaller than the respective values at the other residues. These indicate, that in comparison with other parts, the rigid conformation in this portion plays an important role in the interaction with the enzyme via its Asp residue.

Table 2. ^{13}C chemical shifts and spin-lattice relaxation times for KNI-272 in DMSO-d_6 soln at 300 K

	δ (ppm)	T_1 (s)[a]	NT_1 (s)
iQoa			
Cα	67.23	0.198±0.016	0.396
C—O	167.18	1.080±0.017	
1C	152.25		
3C	142.60		
4C	114.88		
5C	151.85		
6C	110.07		
7C	127.89		
8C	120.07		
9C	127.45		
10C	129.05		
Mta			
Cα	51.22	0.276±0.016	0.276
Cβ	36.12	0.182±0.020	0.364
Cδ	15.13		
C=O	170.02	0.982±0.017	
Apns			
Cα	53.49	0.240±0.015[b]	0.240
Cβ	33.27	0.244±0.021	
Cβ2	71.62		0.244
2,6	129.48		
3,5	128.00		
4	125.99		
1	139.23	1.161±0.014	
C=O	169.49		
Thz			
Cα	62.45	0.280±0.014[b]	0.280
Cβ	33.27		
Cδ	49.44	1.300±0.014	
C=O	168.88		
Bu[i]			
Cα	50.40	3.618±0.007	
Cβ	28.50	0.486±0.003	4.374

[a] T_1 estimated only for the carbons of backbone and C_β.
(±) figures denote the standard deviations.
[b] T_1 could not be estimated because of overlapping signals.

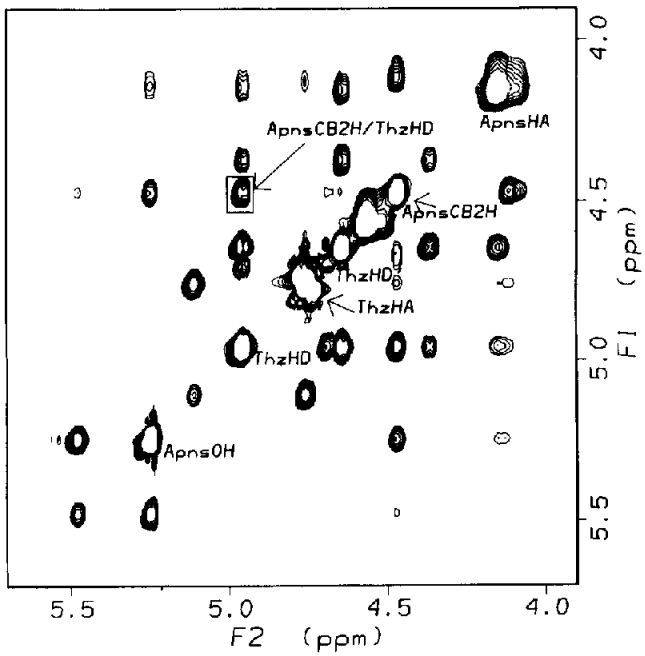

Figure 2. A portion of the ROESY spectra of KNI-272 in DMSO-d_6.

Interproton distances

All observed NOEs in the NOESY spectra were negative, except with those correlations involving phenyl and methyl groups in the side chains. These obviously have additional degrees of motional freedom relative to the backbone in the rest of the molecule. A comparison of NOESY data obtained at mixing times of 300, 400, 500, 600, and 700 ms showed no indication of significant build up of indirect correlations. Thus, it appeared permissible to base a qualitative interpretation of the data upon a classification of the relevant NOEs into categories as strong, medium, and weak for evaluating the NOESY spectrum obtained with the mixing time of 500 ms. All positive NOEs detected at the phenyl and methyl groups in the side chains, which were also observed in ROESY spectrum, were classified as weak. A total of 30 NOEs listed in Table 4 were used for distance restraints.

Structure calculation using simulated annealing approach

A set of 30 structures of KNI-272 were randomly generated using the protocols outlined in the Experimental. Of these resulting structures, five were found to violate the NOE restraints by more than 0.5 Å and thereby were excluded from the final analysis. A superposition of the remaining 25 structures is shown in Figure 3.

Table 3. Coupling constants for KNI-272 in DMSO-d_6 solution at 293 K

Residue	$^3J_{NH-C\alpha H}$ (Hz)	$^3J_{C\alpha H-C\beta H}$ (Hz)
Mta	8.3	5.3, 8.1
Apns	8.1	4.8, 11.0

These structures were analysed in detail and found to fall into three conformational families. Conformers of each class are represented in Figure 4. The relevant torsion angles for those conformers are provided in Table 5. All resulting conformations have a common trans configuration for the Apns—Thz imide bond, and all the ψ_2 torsion angles for the Apns residue have similar values. On the other hand, the primary difference among them is found in the ψ torsion angle for the Apns residues.

Restrained and unrestrained molecular dynamics simulation

The conformation obtained above, which best satisfies the interproton distances and dihedral angles derived from NMR data, was subjected to the restrained molecular dynamics calculation. The trajectories of each dihedral angle of the backbone during this dynamics simulation for 200 ps at 300 K are shown in Figure 5(a). They retain the linear geometry in the backbone from Mta to Apns demonstrating remarkable rigidity in this part. On the other hand, large fluctuations of the ϕ value in iQoa and the ψ value in Thz indicate flexibility of the peptide chain at both the *N*- and *C*-termini.

In the second step of molecular dynamics simulation, the structure was further subjected to 200 ps of unrestrained dynamics at 300 K. The trajectories of the dihedral angles of the backbone during this step are shown in Figure 5(b). Even though they show that the molecule fluctuates more than in the restrained case, the dihedral angles of Mta ϕ and ψ, and Apns ϕ do

Table 4. Summary of inter- and intraresidue NOE distance restraints for KNI-272

NOE	Class[a]
iQoa^{1}C$_\alpha$H-Mta^{2}NH	m
iQoa^{1}C$_\alpha$H-Apns^{3}C$_\alpha$H	w
iQoa^{1}C$_\beta$H-Apns^{3}NH	m
iQoaH4-Mta^{2}C$_\delta$H	w
iQoaH4-Apns^{3}C$_\alpha$H	w
Mta^{2}NH-Mta^{2}C$_\beta$H	m
Mta^{2}NH-Apns^{3}NH	m
Mta^{2}NH-Apns^3-CεH	w
Mta^{2}C$_\gamma$H-Apns^{3}NH	s
Mta^{2}C$_\alpha$H-Mta^{2}C$_\delta$H	w
Mta^{2}C$_\beta$H-Mta^{2}C$_\delta$H	w
Mta^{2}C$_\beta$H-Apns^{3}C$_\delta$H	w
Mta^{2}C$_\delta$H-Apns^{3}C$_\alpha$H	w
Apns^{3}NH-Mta^{2}C$_\delta$H	w
Apns^{3}NH-Apns^{3}C$_\beta$H	s
Apns^{3}NH-Apns^{3}C$_{\beta 2}$H	m
Apns^{3}NH-Apns^{3}C$_\alpha$H	w
Apns^{3}NH-Mta^{2}C$_\delta$H	w
Apns^{3}C$_\alpha$H-Apns^{3}C$_\delta$H	w
Apns^{3}C$_\alpha$H-Apns^{3}C$_\beta$H	w
Apns^{3}C$_\alpha$H-Thz^{4}C$_\delta$H	m
Apns^{3}C$_\beta$H-Apns^{3}OH	m
Apns^{3}C$_\beta$H-Apns^{3}C$_{\beta 2}$H	m
Apns^{3}C$_\beta$H-Apns^{3}C$_\alpha$H	w
Apns^{3}C$_\beta$H-Apns^{3}C$_\varepsilon$H	w
Apns^{3}C$_{\beta 2}$H-Thz^{4}C$_\delta$H	m
Apns^{3}C$_\alpha$H-Bu^{t4}C$_\beta$H	w
Apns^{3}C$_\varepsilon$H-Bu^{t4}C$_\beta$H	w
Thz^{4}C$_\beta$H-Thz^{4}C$_\delta$H	w

[a]s, m, and w refer to strong, medium, and weak NOEs, respectively.

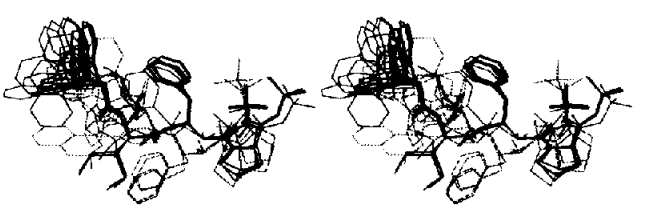

Figure 3. Superposition (backbone atoms only) of the 25 structures generated by the simulated annealing procedure for KNI-272.

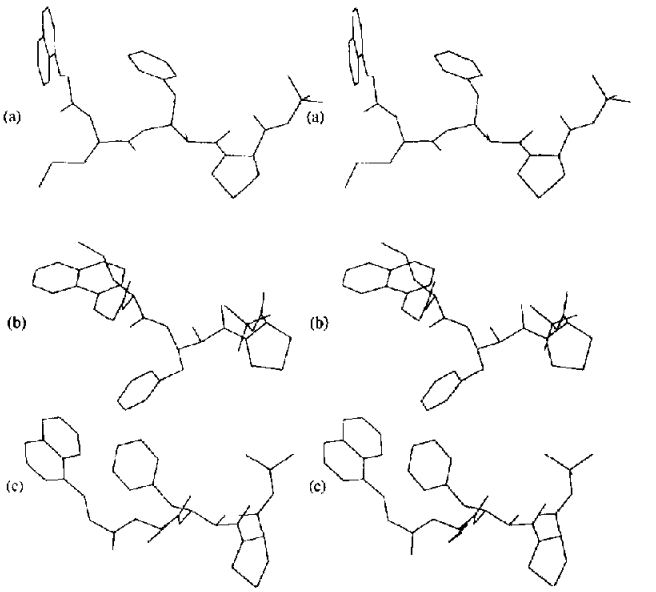

Figure 4. Stereoview of three representative conformers (A, B, and C).

Table 5. Torsional angles of three representative conformers (A, B, and C) of KNI-272

Residue	Conformation A	Conformation B	Conformation C
iQoa			
ψ	58.39	130.12	59.00
χ^1	179.54	77.97	179.58
Mta			
ϕ	−145.37	−144.15	−145.09
ψ	80.08	84.91	79.44
χ^1	−65.56	−65.89	−65.60
Apns			
ϕ	−111.16	−114.36	−110.75
ψ	166.83	−58.68	71.88
ψ^2	−73.29	−94.08	−92.89
χ^1	−72.96	−66.86	−73.69
Thz			
ϕ	68.71	−80.29	−70.49
ψ	138.40	−48.09	120.48
χ^1	−27.03	39.57	−23.01

not change so much, indicating that the backbone of the peptide around these residues has a fairly rigid conformation.

Discussion

In this work, we used DMSO-d_6 as a solvent for NMR measurement. Although the solvent undoubtedly plays a role in determining structure, we noted that Baldwin et al.[6] had reported that all single structures obtained from various solvents were similar to the bound structure. Hence, the constraint or predisposition toward the active conformation appears stronger than particular solvent or crystal interactions. It would be good to analyse the structure in an aqueous environment, if it were practical. However, it would be worthwhile to point out that there are the opinions and discussion of the similarities of the dielectric constant of DMSO to that of the inner parts of proteins or ligand–protein interfaces.[10,11]

In order to evaluate the NOESY crosspeaks, we classified them roughly into three classes (i.e., strong, medium, and weak). As stated earlier, the NOESY spectrum observed in the DMSO-d_6 solution exhibited both positive and negative peaks, and intensities of NOESY crosspeaks were so weak as to prevent accurate volume integrations. Since a short linear peptide such as KNI-272 undergoes conformational averaging in solution, the measured NOEs for such a peptide show averaged values over all the accessible conformational space of the molecule within the time scale of magnetic relaxation. Thus, the commonly used assumption that the whole molecule has a unique correlation time, and that identical density functions are applicable for all protons, was considered to be inappropriate for KNI-272. For these reasons, extraction of more accurate interproton distances from the NOESY spectrum was not attempted.

Due to the lack of distance information and, as a result, the lack of the distance constraints during the calculation, the structures resulting from the simulated annealing calculation did not converge to a unique structure and were found to be distributed into three families as shown in Figure 4. The wide variety of the conformers comes mainly from the diverse values of the dihedral angle ψ in the Apns residue that directly reflects the fact that distance information was missing around the C_α and $C_{\beta 1}$ bond of this residue. The typical values listed in Table 5 reveal that the configuration around this angle should be *trans* in the conformation A and *gauche* in the conformations B and C, respectively. The HMBC spectrum is generally expected to differentiate among these configurations, because it may give rise to the signal for spin–spin coupling between the carbon nucleus of $C_{\beta 1}$ and the proton of $C_{\beta 2}$. Actually, the cross peak for the coupling was found in the spectrum of KNI-272 as shown in Figure 6. Judging from its strong peak intensity, the dihedral angle is likely to be close to 0 or 180° and the configuration, therefore, is in the *trans* form. This information makes it clear that the conformer A is the best candidate of the three conformers for the solution structure of KNI-272.

Surprisingly, conformation A is close to the single-crystal structure and also similar to the binding structure of that complexed with protease as determined by X-ray analysis. All three structures are superimposed in Figure 7. Although the iQoa residue did not converge into a superimposable or unique structure, the hydroxyl and the carbonyl groups of the Apns residue were superimposable. Thus the structure of this latter part of the molecule is fixed in the active state in all three conditions and this result strongly supports the 'pre-organization' hypothesis. Small T_1 values related to these important groups also supports rigidity in this part of the molecule and gives credence to the hypothesis as well.

Before the X-ray structural analysis of the protease complex was resolved, we had begun to characterize the conformation of KNI-272 in solution using NMR spectroscopy. During the process of the lead compound

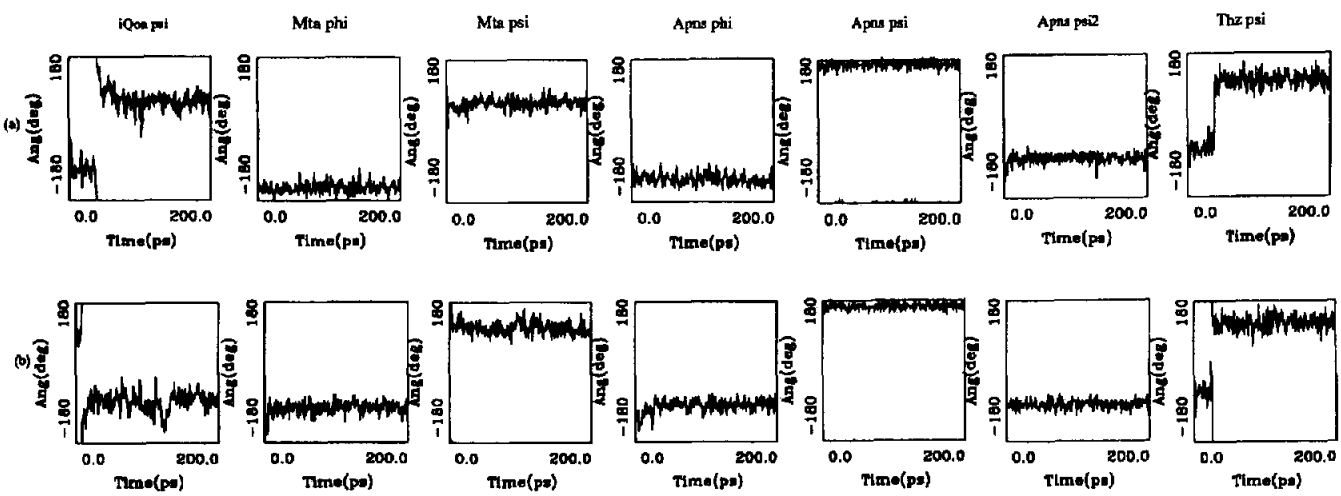

Figure 5. Variations of dihedral angles of the backbone of KNI-272 during the 200 ps dynamics simulations. (a) restrained and (b) unrestrained simulation.

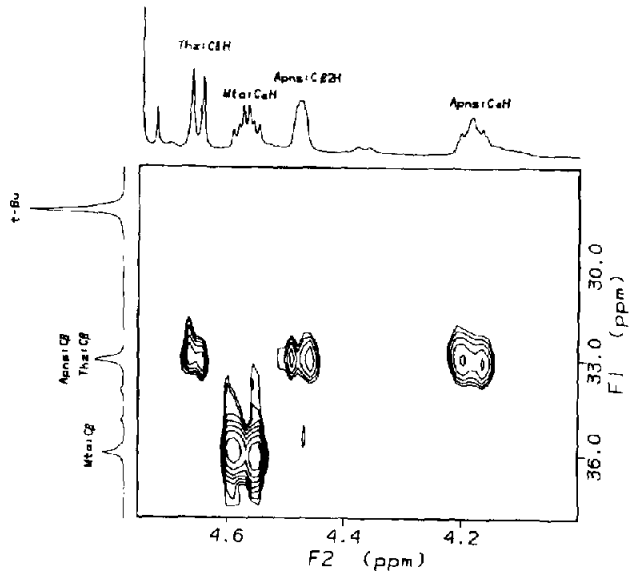

Figure 6. Portions of ^1H ^{13}C HMBC spectra of KNI-272 in DMSO-d_6.

optimization, this NMR study provided important information to improve the synthetic design. In particular, it was interesting to know which configuration is preferred, *trans* or *cis*, about the imide bond between the Apns and Thz residues. Although the *trans* isomer is known to be dominant for natural amino acids, it was hard to predict the preference for such a nonnatural occurring amino acids. Here the ROESY spectra revealed the coexistence of both isomers and showed that the *trans* was more prevalent.

We hypothesized that the degree of preference would correlate with the activity of the compound and synthesized a series of tripeptides with a sequence of Z-Asn-Apns-X-NHBu^t (e.g., KNI-102, KNI-125, and KNI-164) where Xs are Pro, Thz (thioproline) and Dmt (dimethylthioproline), respectively. The inhibitory activity of each compound was tested to show that IC_{50} is 89 nM for KNI-102, 31 nM for KNI-125, and 3.5 nM for KNI-164, respectively.[1] We calculated the *trans/cis* ratios in these compounds from the peak intensities of C_α carbon using NMR and found that they are 0.15, 0.19, and 0.15, respectively. Then we calculated the energy barrier about the peptide bond between the

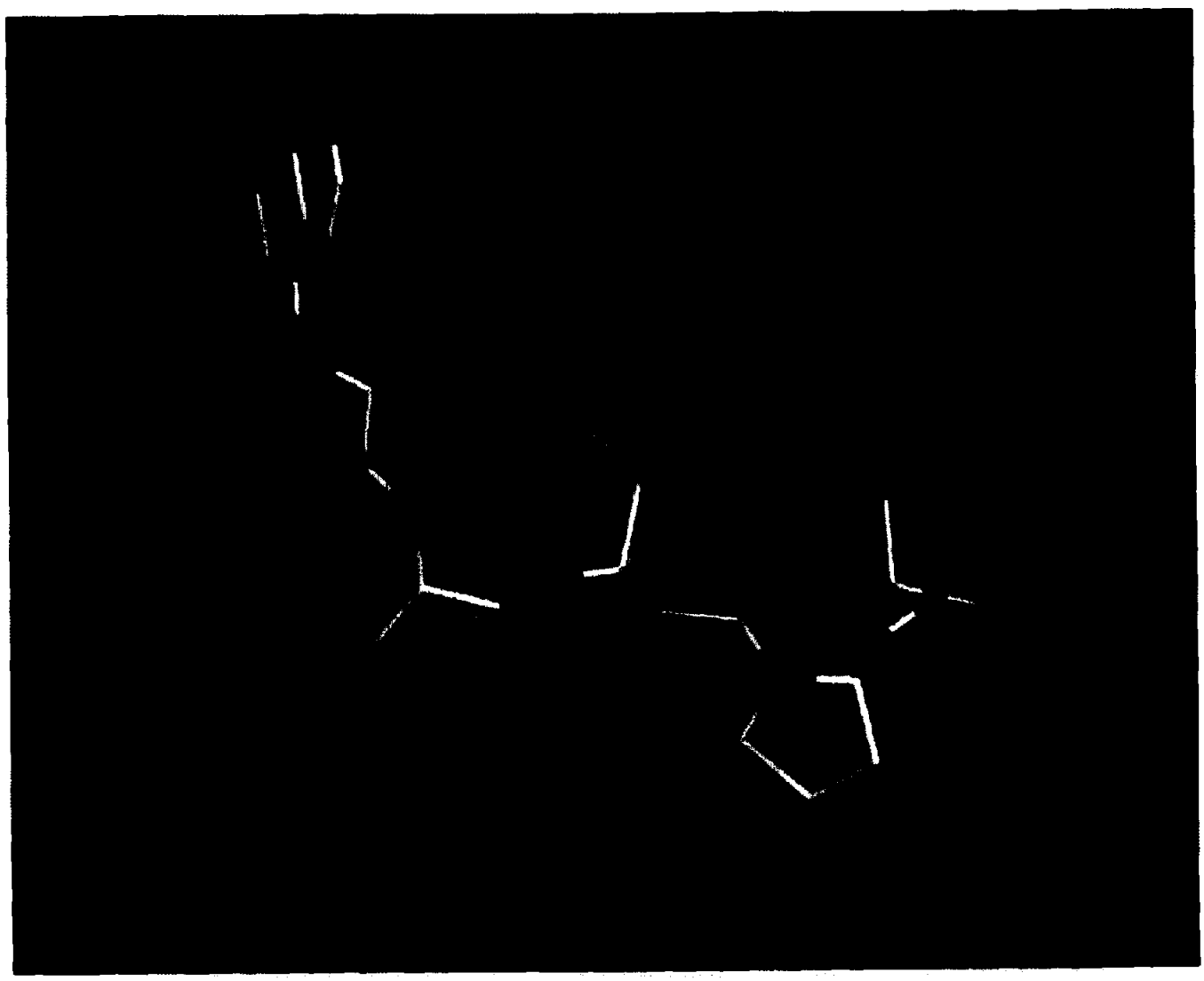

Figure 7. Superposition of KNI-272 structures: in solution is shown coloured by atom type, in single crystal is purple, and in complex is orange.

cis/trans isomers for each compound using the grid search method. However, we did not find any distinct differences among them. Thus, we concluded that there is no direct relation between the inhibitory activity and the *trans/cis* ratio.

Since we failed to find a correlation between inhibition and isomer type, we were motivated to carry out the conformational analysis on KNI-272. The NMR-based approach often has limitations in the determination of structure for short oligopeptides in solution. Structure cannot always be determined from the observed NOESY data and their distant constraints alone. We could not delineate a unique structure for KNI-272 without resorting to additional established techniques and other information, ^{13}C relaxation and HMBC measurements.

The result showed that the both the structure of KNI-272 in the solution and that in the single crystal are similar. Furthermore it showed the same structures in solid regardless of which solvents were used for growing crystals. Finally, the structure in the inhibitor–protease complex, as determined by the X-ray analysis, is the same as these structures determined by the solution NMR. This led us to conclude that the solution and solid-state structures are the same. Since the structures in solution and solid state are the same, it follows that the rigid conformation of this ligand is also its bioactive form.

Conclusion

The solution conformation of a HIV protease inhibitor, KNI-272, was found to be similar to that for both the ligand in single crystal and in the crystalline ligand–enzyme complex. The backbone from Mta to Apns, which plays an important role in the interaction of the ligand (inhibitor) with the enzyme via its Asp residue, showed remarkable rigidity or appears fixed in the active form. The fact that KNI-272 exists freely in solution, and is an active form, strongly supports the 'preorganization' hypothesis.

Experimental

NMR spectroscopy

The HIV protease inhibitor, KNI-272, was synthesized and then purified by reverse-phase HPLC as described previously.[1] The samples were dissolved in DMSO-d_6 at various concentrations (1–100 mM). For the NOE and T_1 experiments, the solutions were freshly degassed by freeze–thaw–pump cycles.

NMR experiments were initially recorded on General Electric QE-300 and Omega 500 spectrometers, and later experiments were carried out on a Bruker AMX500. Chemical shifts are referenced to internal DMSO set at 2.49 ppm for proton and 39.5 ppm for carbon. ^1H 1-D spectra were acquired for a 4 mM sample with 32 K data size at 293 K; 100 mM sample and 64 K data were used for ^{13}C experiments at 300 K. For both homo- and hetero-correlated 2-D experiments, standard pulse programs from the GE and Bruker software libraries were used. All 2-D spectra, except the HMBC experiment, were recorded in the pure-phase absorption mode according to the time-proportional phase increment (TPPI).

NOESY and ROESY spectra were acquired with mixing times from 300 to 700 ms. Spin diffusion effects on NOE cross peaks were checked by the build-up curve.

All NMR data sets were processed with FELIX software distributed by Biosym on a SGI 4D/35 workstation.

Simulated annealing

A model structure for KNI-272 was built and manipulated with INSIGHTII software distributed by Biosym on a SGI 4D/35. Minimization and molecular dynamics were performed with the CVFF with the DISCOVER program from Biosym. A cut off distance of 10 Å was used for nonbonded interactions. Distance restraints for the lower limit were fixed at 1.8 Å, and for upper limit, the distances elucidated from the NOESY spectrum with a 500 ms mixing period were given according to the intensities of NOE, i.e., 2.5 Å for a strong NOE crosspeak, 3.5 Å for a medium, and 4.5 Å for a weak NOEs, respectively. Pseudoatoms defining the centroids of the aromatic rings, methyl groups, and *tert*-butyl groups were introduced to correct the interproton distances.[12] All peptide bonds were constrained to the *trans* configuration. Pseudoforce constants for NOE, coupling constant, peptide bond were set to 15 kcal/mol Å^2, 30 kcal/mol rad^2, and 50 kcal/mol rad^2, respectively.

The simulated annealing calculation used in this study consists of the following 14 separated phases.[13] The first phase involved randomization of all atomic coordinates followed by steepest-decent minimization of the starting structures using quadratic potentials and very low force constants for each term of the pseudoenergy function, including chiral and NOE constraints. The second phase involved additional minimizations with 1500 iterations of conjugate-gradient minimization. Phases 3–5 involved simulated annealings with increased scaling of the force constants up to their full values. Phases 6–10 involved cooling of the molecule from 1000 to 300 K over 10 ps. The final phases involved minimization using the steepest-decent and conjugate-gradient algorithm with Leonard–Jones potentials.

The structure that best satisfied the distance and the dihedral angle constraints derived from the NMR data was subjected to 200 ps of restrained dynamics at 300 K. For this simulation, the maximum force was set at 10 kcal/mol^{-1}, and the force constant was set at 3 kcal mol/Å^2. Molecular geometries were stored at 1 ps intervals during the dynamics run to render a set of 200

structures. Unrestrained dynamics starting from the same structure to the above initial structure were also performed at 300 K.

Acknowledgments

We would like to thank Dr J. Erickson for providing the coordinates of KNI-272 complexed with enzyme and Dr T. Ishida for providing the coordinates of crystalline KNI-272. We also thank Messrs N. Nemoto and K. Miyazaki, who carried out the initial experiments. Y. O. is grateful to Shimadzu Corporation (Kyoto) for support of this research.

References

1. Mimoto, T.; Imai, J.; Kisanuki, S.; Enomoto, H.; Hattori, N.; Akaji, K.; Kiso, Y. *Chem. Pharm. Bull.* **1992**, *40*, 2251.

2. Mimoto, T.; Imai, J.; Tanaka, S.; Hattori, N.; Kisanuki, S.; Akaji, K.; Kiso, Y. *Chem. Pharm. Bull.* **1991**, *39*, 3088.

3. Iizuka, K.; Kamijo, T.; Harada, H.; Akahane, K.; Kubota, T.; Umeyama, H.; Ishida, T.; Kiso, Y. *J. Med. Chem.* **1990**, *33*, 2707.

4. Kageyama, S.; Mimoto, T.; Murakawa, Y.; Nomizu, M.; Ford Jr. H.; Shirasaka, T.; Gulnik, S.; Erickson, J.; Takada, K.; Hayashi, H.; Broder, S.; Kiso, Y.; Mitsuya, H. *Antimicrob. Agents Chemother.* **1993**, *37*, 810.

5. Doi, M.; In, Y.; Ishida, T.; Kato, R.; Takahashi, O.; Erickson, J.; Mimoto, T.; Kiso, Y., to be published.

6. Baldwin, E. T.; Bhat, T. N.; Gulnic, S.; Liu, B.; Topol, I. A.; Kiso, Y.; Mimoto, T.; Mitsuya, H.; Erickson, J. W. *Structures* **1995**, *15*, 581.

7. Nicklaus M.C.; Wang, S.; Driscoll, J. S.; Milne, G. W. *Bioorg. Med. Chem.* **1995**, *3*, 411.

8. Wüthrich, K.; Billeter, M.; Braun, W. *J. Mol. Biol.* **1984**, *180*, 715.

9. Allerhand, A.; Doddrell, D.; Komoroski, R. *J. Chem. Phys.* **1971**, *55*, 189.

10. Motta, A.; Morelli, M. A. C.; Goud, N.; Temussi, P. A. *Biochemistry* **1989**, *28*, 7996.

11. Motta, A.; Temussi, P. A.; Wünsch, E.; Bovermann, G. *Biochemistry* **1991**, *30*, 2364.

12. Wüthrich, K.; Billeter, M.; Braun, W. *J. Mol. Biol.* **1983**, *169*, 949.

13. Clore, G. M.; Brunger, A. T.; Karplus, M.; Groneborn, A. M. *J. Mol. Biol.* **1985**, *191*, 435.

(*Received in U.S.A. 27 October* 1995)